Chemical Physics Letters 775 (2021) 138687

Contents lists available at ScienceDirect

Chemical Physics Letters

journal homepage: www.elsevier.com/locate/cplett

Research paper

Ionization – dissociation of methane in ultrashort 400 nm and 800 nm laser fields

Lazaros Varvarezos [a,*], John T. Costello [a], Conor Long [b], Alexander J. Achner [c], Rene Wagner [c], Michael Meyer [c], Patrik Grychtol [c]

[a] Dublin City University, School of Physical Sciences and NCPST, Dublin 9, Ireland
[b] Dublin City University, School of Chemical Sciences, Dublin 9, Ireland
[c] European XFEL, Holzkoppel 4, 22869 Schenefeld, Germany

ARTICLE INFO

Keywords:
Molecular dissociation
Methane
Laser fields

ABSTRACT

The effect of laser wavelength on the dissociation mechanisms in methane is examined over a broad range of intensities for both 800 nm and 400 nm laser fields. It is found that, at lower laser intensities, the dissociation pathways identified with the aid of theoretical calculations for the methane cation can account for most of the experimental findings, including the differences observed for irradiation by 800 nm and the 400 nm fields. As the laser intensity increases, the significance of the Coulomb explosion mechanism, along with the contribution of the rescattering process and the concomitant dissociation pathways, is highlighted.

1. Introduction

Methane, the simplest member of the hydrocarbon family, has attracted special attention primarily due to its role as the most significant contributor to the greenhouse effect [1,2] and it's consequent climatic and economic impacts [3]. Furthermore, being the second most abundant compound in Titan's atmosphere, methane is considered a benchmark molecule in astrophysics [4,5]. For example, in the case of Titan, when ultraviolet radiation emitted by the Sun interacts with methane, complex hydrocarbons are formed in its upper atmosphere. In order to unveil the nature of such photochemical reactions a deep understanding of the most fundamental light induced processes such as the ionization and subsequent dissociation of methane is essential.

Table-top lasers, providing pulses of short (ps) and ultrashort (fs) duration, have been extensively used in order to induce and probe molecular fragmentation [6–8]. Such investigations have revealed several fascinating phenomena. For example, charge resonance enhanced ionization (CREI) [9–12], observed in diatomic molecules [13–19], is a model case of the interplay between electronic and nuclear degrees of freedom. Importantly, understanding of these mechanisms is a first step towards the control of molecular dissociation [20,21].

The situation becomes even more intriguing when one transitions from diatomic molecules to small polyatomic molecules, such as methane, where fragmentation patterns become more complex. For that reason, the interaction of methane with laser fields has been studied extensively and for a wide variety of experimental parameters. For example, Cornaggia and Hering [22] observed the production of multicharged atomic ions upon Coulomb explosion of methane irradiated by high intensity (10^{15}–10^{16} W/cm^2), ultrashort (27 fs) laser pulses at a central wavelength of 800 nm. On the other hand, a study performed by Mathur and coworkers [23], utilizing significantly longer pulses (35 ps) at a wavelength of 532 nm resulted in the absence of the CH_3^+ signal from the time of flight (TOF) ion spectrum for intensities of the order of 10^{14} W/cm^2. At an even longer pulse duration of 7 ns, and for a laser wavelength of 532 nm, Chen et al. [24] reported the absence of the CH_4^+ fragment from the ion spectrum at laser intensities of $\approx 10^{13}$ W/cm^2. This finding was proposed to arise from the high rate of dissociation of CH_4^+ into the CH_3^+ and a hydrogen atom. Conversely, when the pulse duration was reduced to 8 fs [25], all of the fragment ions disappeared, except for the CH_4^+ and CH_3^+ molecular ions, indicating that methane did not stay long enough in the laser field to trigger dissociation after the ionization step

Two alternative mechanisms have been proffered in the literature in order to explain the dissociation of methane. On one hand the so-called field assisted dissociation (FAD) model along with the quasi classical trajectory calculation [26–28], is based on the hypothesis that the potential energy curves along the C-H bond are preferentially distorted by the laser field along the polarization direction, in such a way as to favour

* Corresponding author.
E-mail address: lazaros.varvarezos2@mail.dcu.ie (L. Varvarezos).

https://doi.org/10.1016/j.cplett.2021.138687
Received 8 April 2021; Received in revised form 22 April 2021; Accepted 23 April 2021
Available online 28 April 2021

the $CH_4^+ \rightarrow CH_3 + H^+$ channel over the $CH_4^+ \rightarrow CH_3^+ + H$ pathway. The same holds for the other dissociation channels (e.g., the $CH_3^+ \rightarrow CH_2 + H^+$/$CH_3^+ \rightarrow CH_2^+ + H$ pathway and so forth). In these works, only the ground state of the molecular ion was considered and only for ultrafast (160 fs) laser pulses at 800 nm and intensities in the range of 10^{13} –10^{14} W/cm^2, as used in the experiments [26–28]. An alternative stepwise dissociation process was revealed in a later experiment [29] performed using 800 nm laser pulses of 48 fs duration at intensities on the order of 10^{14}–10^{15} W/cm^2. In that case: $CH_4^+ \rightarrow CH_3^+ + H$, $CH_3^+ \rightarrow CH_2^+ + H$, $CH_2^+ \rightarrow CH^+ + H$, $CH^+ \rightarrow C^+ + H$ were all proposed to be the dominant dissociation pathways. From a physical standpoint, the difference between the two aforementioned studies (i.e., Refs. [26–28] and Ref. [29]) is that the former dissociation occurs within the spatio-temporal influence of the laser pulse, whereas in the latter case the laser pulse is assumed to generate hot and unstable ions which subsequently dissociate. Thus, it seems possible that one can use a combination of pulse duration and laser intensity to favour one of the two alternative dissociation scenarios over the other. While the FAD model and the stepwise process provide a qualitative description of the C-H bond cleavage, some important questions remain unanswered. Principal among these is how a particular C-H bond of the four equivalent C-H bonds in methane is selected for cleavage. Secondly, the model presented in [29] does not provide any information on the effect of laser wavelength on the efficiency of the fragmentation nor the product distribution.

In this work ultrashort pulse duration (35 fs) with moderate laser intensities, below 10^{15} W/cm^2 are used in order to examine the dissociation of methane in a different set of experimental conditions with respect to the abovementioned studies [26–29]. In addition, measurements are also performed using the second harmonic of the fundamental laser wavelength at 400 nm leading to a direct comparison of the fragmentation patterns for the two laser wavelengths. To the best of our knowledge, such a comparative study on methane dissociation has not been reported in the literature to date. Besides understanding of the fundamental dissociation processes, this study aims to provide a first step towards controlling the dissociation pathways in CH_4 by carefully selecting the laser parameters.

2. Experiment

The experiments were performed using the laser system installed in the laboratory of the SQS (Small Quantum Systems) research group at the European XFEL, which is a Ti:Sapphire based system incorporating two amplification stages (Coherent Legend Duo). This arrangement provided high average power (10 W) along with pulses of ultrafast duration (~35 fs measured by a Frequency Resolved Optical Gating FROG autocorrelator [30]) at a repetition rate of 3 kHz and a wavelength centered at 800 nm. A long focal length (1400 mm) lens, followed by a gold coated, toroidal mirror with an effective focal length of 400 mm, were used to focus the laser beam down to a 50 μm diameter beam waist in the interaction region. The laser was incident on the focusing mirror at an incidence angle of ~ 70°. In order to facilitate intensity dependent measurements, a motorized attenuator was used. It comprised a half wave plate followed by two polarizers set at an angle of incidence of ~72°. The second harmonic radiation was generated with an efficiency of ca. 35%, by means of a Type I BBO crystal and two ultrafast harmonic beam splitters. The pulse duration for the 400 nm beam was comparable to that of the fundamental laser. The transmission was adjusted, to achieve comparable intensities between the 800 nm and the 400 nm fields in the interaction region. Under these conditions, the intensities present in this experiment varied between 0.8×10^{14} W/cm^2 and 7.0×10^{14} W/cm^2 for both the fundamental laser wavelength and the second harmonic.

The gas target was injected by means of an effusive gas needle. The chamber was pumped down to a base pressure of 1×10^{-9} mbar. The typical operating pressure was on the order of 1×10^{-8} mbar, low enough to minimize any contribution to the signals coming from space charge effects in the interaction region. The measurements presented in this work, were taken using the TOF spectrometer housed in the SQS experimental chamber, which is based on the well-established the Wiley-McLaren design [31]. Background spectra were recorded to ensure the absence of contaminants in the chamber.

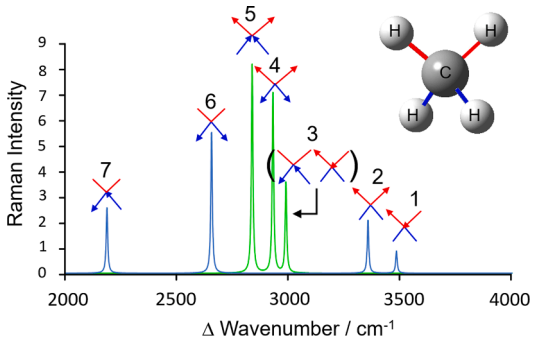

Fig. 1. The C-H stretching normal modes of CH_4^+ with strong bonds in red and weak bonds in blue, the green spectrum is the calculated Raman spectrum in the absence of an applied electric field while the blue spectrum was calculated in the presence of an electric field. The red and blue vectors indicate the relative displacement of the hydrogen atoms in the vibration in each normal mode 1–7; mode 3 is degenerate as indicated by the two sets of displacement vectors in parentheses.

3. Theory

The calculations were performed using the Gaussian 16 program suite [32] (Revision B.01) at the Irish Centre for High-end Computing (ICHEC). Unrestricted Hartree-Fock level calculations were performed with the 6-31G basis set [33,34]. The optimized geometry of the CH_4^+ was calculated at a range of electric field intensities by using the Field parameter [35]. The vibrational spectra were computed and the absence of negative eigenvalues confirmed that the optimized geometry was located at a minimum on the potential energy hypersurface. The Raman spectrum was constructed in the presence and absence of an applied electric field. It should be noted that quantum chemical calculations in this work can only model homolytic cleavage and in the case of cleavage of C-H bonds in CH_4^+, the calculations cannot account for the production of H^+ which would require subsequent ionization of the H or H_2 products by the laser field.

From a theory standpoint, the approach adopted in this work differs fundamentally from that reported earlier (e.g., in [25]). Thus, instead of arbitrarily selecting one of the four equivalent C-H bonds in methane for manipulation in the electronic ground-state of the CH_4^+, the motions along the normal vibrational modes of CH_4^+ which involve C-H stretching were modelled in the presence of an external electric field. Ionization of CH_4 to CH_4^+ results in a small but significant structural change. The four C-H bonds are no longer symmetry related (indistinguishable) and the cation has two sets of two symmetry-related C-H units. The cation possesses a two-fold proper rotation along with a vertical plane of symmetry and therefore belongs to the C_{2v} point group [36]. The consequence of this reduced symmetry, compared to the neutral

Table 1
The optimised C-H bond distance for CH_4^+ in different laser intensities at the UHF/6-31G level.

Laser Intensity (W/cm^2)	C-H Distance (Å)	
	Weak Bonds	Strong Bonds
0	1.11069	1.11067
3.50×10^{12}	1.16977	1.07273
3.50×10^{13}	1.16981	1.07266
1.10×10^{14}	1.16999	1.07252
1.40×10^{14}	1.17009	1.07245

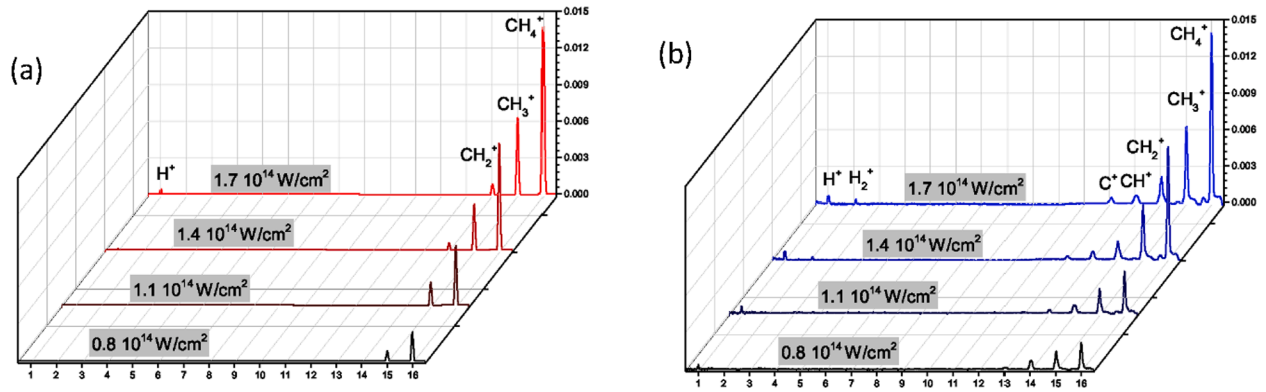

Fig. 2. (a) Ion TOF spectra as a function of the laser intensity for dissociation of methane irradiated by 800 nm laser pulses in laser intensities ranging between 0.8 × 10^{14} W/cm^2 and 1.7 × 10^{14} W/cm^2. (b) Same spectra for irradiation with 400 nm laser pulses, obtained for comparable laser intensities.

methane, is to increase the number of vibrational degrees of freedom. For instance, neutral methane exhibits two C-H stretching modes in its Raman spectrum, while this increases to three for the CH_4^+ in the absence of an external field (Fig. 1, green spectrum), and four when an external field is applied (Fig. 1 blue spectrum). These spectra are superimposed in Fig. 1 together with a representation of the associated normal vibrational modes and a ball and stick model of CH_4^+ in the orientation of the normal mode representations.

From these calculations it is clear that increasing the electric field strength increases the distortion of the cation from tetrahedral geometry resulting in a lifting of mode degeneracy (see Table 1 below). This permits the modes to be defined in terms of the motion of the strong (red) or weak C-H bonds (blue) as represented in the displacement vectors in Fig. 1. The bond lengths of the two sets of symmetry related C-H units at equilibrium geometry are presented in Table 1. The normal modes identified in these calculations were used as the basis for a series of potential energy scans under different laser intensities. The normal modes selected for these studies were all the C-H stretching modes modelled in the presence of an electric field, i.e. modes 1, 2, 6, and 7 in addition to the totally symmetric stretch which is only observed in the absence of an electric field (mode 4). Each mode was modelled along a reaction coordinate, which for instance for the symmetric modes 2 and 6 consists of the concerted stretch of the strong and weak C-H bonds, respectively. Thus, the mode can be represented by a single C-H distance along the reaction coordinate. The asymmetric modes 1 and 7 were represented by a single C-H distance from a distance shorter than the equilibrium distance to one which is extended beyond the cleavage of the C-H bond. In these potential energy scans, all remaining structural parameters were optimized at each point along the reaction coordinate in a relaxed potential energy scan. Modes 3 and 5, active in the absence of an applied field, have their equivalence in modes 1 and 7 and modes 2 and 6 respectively in the presence of an external field.

4. Results and discussion

The time of flight (TOF) mass spectra obtained following exposure of CH_4 to an 800 nm pulse at laser intensities ranging from 0.8 to 1.7 × 10^{14} W/cm^2 are presented in Fig. 2(a). For intensities less than 1.1 × 10^{14} W/cm^2, peaks corresponding to the CH_4^+ and CH_3^+ are observed while the CH_2^+ feature appears only for intensities greater than 1.1 × 10^{14} W/cm^2. A peak corresponding to H^+ is observed when the laser intensity reaches ≈1.7 × 10^{14} W/cm^2 which is slightly higher than that measured by Wang and co-workers [26]. The absence of signals associated with contaminant impurities (e.g., H_2O) confirms that the dissociation of CH_4 is the dominant source of H^+ in these experiments.

The ion TOF spectra for the second harmonic laser field (400 nm) obtained under comparable conditions are presented in Fig. 2(b). In these experiments the H^+ peak is evident even at the lowest laser intensity, together with the CH_4^+, CH_3^+, CH_2^+ and CH^+. Peaks corresponding to C^+ and H_2^+ ions emerge at a laser intensity of ≈1.4 × 10^{14} W/cm^2. These species are not observed with 800 nm laser pulses in this intensity range.

These experiments confirm that the extent of fragmentation is considerably greater for 400 nm pulses compared to 800 nm pulses of similar intensities. Quantum chemical calculations have been applied to explain these differences. The optimized structure of the CH_4^+ ion was used as the starting point for these calculations and this allowed the identification of the normal vibrational modes or internal degrees of freedom of the ion. These normal modes will interact with the oscillating electric field vector of the incident pulse resulting in progression of each normal mode to higher vibrational quantum levels. This progression up the vibrational quantum levels will be greater for a 400 nm pulse compared to an 800 nm pulse, simply because the number of cycles to which the CH_4^+ is exposed to is greater for 400 nm pulses compared to 800 nm pulses. This ultimately results in breaking of one or more C-H bonds and the formation of some of the fragment ions as observed in the TOF spectra. To explain the fragmentation, the normal modes 1, 2, 4, 6,

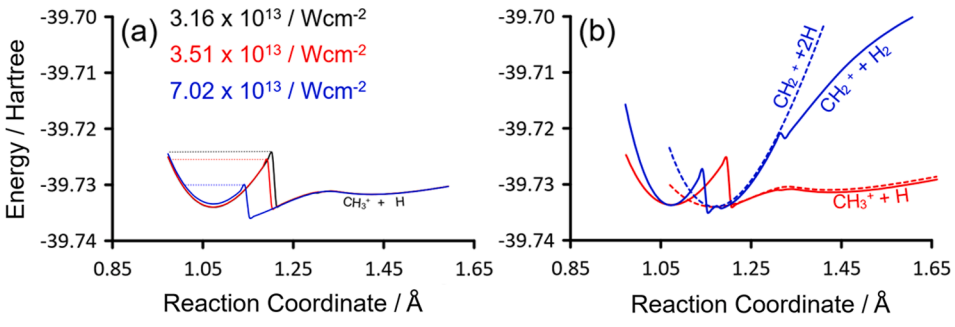

Fig. 3. (a) The potential energy profiles along the antisymmetric stretch of the strong bonds in CH_4^+ leading to CH_3^+ and H (mode 1), for three different laser intensities, the sharp energy drop occurs at the recoil point where the CH_3^+ fragment undergoes spontaneous structural change. (b) A comparison of the potential energy profiles of the antisymmetric (mode 1 solid red, and mode 7 dashed red, curves) and symmetric (mode 2 dashed blue, and mode 6 solid blue, curves) respectively at the same field intensity (3.51 × 10^{13} W/cm^2).

Table 2
The dissociation pathways induced by progression along various normal modes.

Mode No.	Induced Reaction
1	$CH_4^+ \rightarrow CH_3^+ + H$
2	$CH_4^+ \rightarrow CH_2^+ + H_2$
4	$CH_4^+ \rightarrow C^+ + 2H + H_2$
6	$CH_4^+ \rightarrow CH_2^+ + H_2$
7	$CH_4^+ \rightarrow CH_3^+ + H$

and 7 were followed to extreme values of C-H displacements for different electric field strengths. Each of these calculations provide a potential energy profile along the reaction coordinate leading to fragmentation. For example, in Fig. 3 (a) the potential energy profile along mode 1 leading to CH_3^+ and H formation is presented for three field strengths. As can be seen, the potential well close to the equilibrium geometry mimics that of a simple harmonic oscillator up to a point where the CH_3^+ fragment undergoes a structural change. We have called this the recoil point where the energy drops precipitately as the structure of the CH_3^+ fragment relaxes. This recoil point is important for a number of reasons. Firstly, the recoil releases considerable potential energy as kinetic energy causing, in this case, the CH_3^+ and H fragments to fly apart. Secondly, the progression along the potential energy profile is fully reversible up to the recoil point but subsequent to the recoil the reaction becomes irreversible. Thirdly, after the recoil and the relaxation of the carbon-containing fragment, the system is no longer constrained to motion along the selected normal mode of the CH_4^+ ion. The fragmants can diffuse apart or further react in the case of H_2. The location of the recoil point depends on the field strength, the higher the field strength the lower the energy at recoil. Fig. 3(b) compares the energy changes along modes 1,2,6, and 7. What is noticeable here is the very low barrier to CH_3^+ formation in mode 7, the asymmetric stretch of the weak bonds (red dashed curve). This explains why CH_3^+ is observed in all TOF spectra in this work, irrespective of the laser intensity or laser wavelength (Fig. 2). The recoil point on the symmetric stretch (solid blue curve forming CH_2^+ fragments) exhibits a rather low barrier, explaining why the CH_2^+ fragment is observed in all TOF spectra using the 400 nm laser. A field strength of 1.4×10^{14} W/cm^2 is required for CH_2^+ to be observed using an 800 nm laser pulse, as progression up the vibrational quantum levels is greater for the second harmonic field.

The resulting reactions associated with each normal mode are presented in Table 2.

Fig. 4(a) and 4(b) represent the ion TOF spectra obtained at higher laser intensities for both the fundamental and the second harmonic laser fields respectively. In that case, the fragmentation pattern becomes significantly different compared to what we observe at lower intensities for both the fundamental laser wavelength and the second harmonic case. The most striking difference concerns the H^+ ions in the TOF spectra. More specifically, at higher laser intensities the relative H^+ signal associated to the 800 nm laser field is significantly stronger compared to the case of the second harmonic field within the same intensity region. Fig. 5 (a) and 5 (b) focus on the region of H^+ fragment associated with the spectra shown in Fig. 4 (a) and (b) respectively.

Importantly, Fig. 5(a) shows that, for the case of 800 nm laser field, the H^+ fragments exhibit forward–backward peaks which are indicative of ions carrying high kinetic energy. This is a noteworthy difference compared to lower laser intensities, implying that the H^+ ions cannot be attributed to the same dissociation process invoked earlier for that lower intensity range. Instead, ions carrying significant kinetic energies, on the order of several eV's, should be considered as products of a Coulomb explosion process.

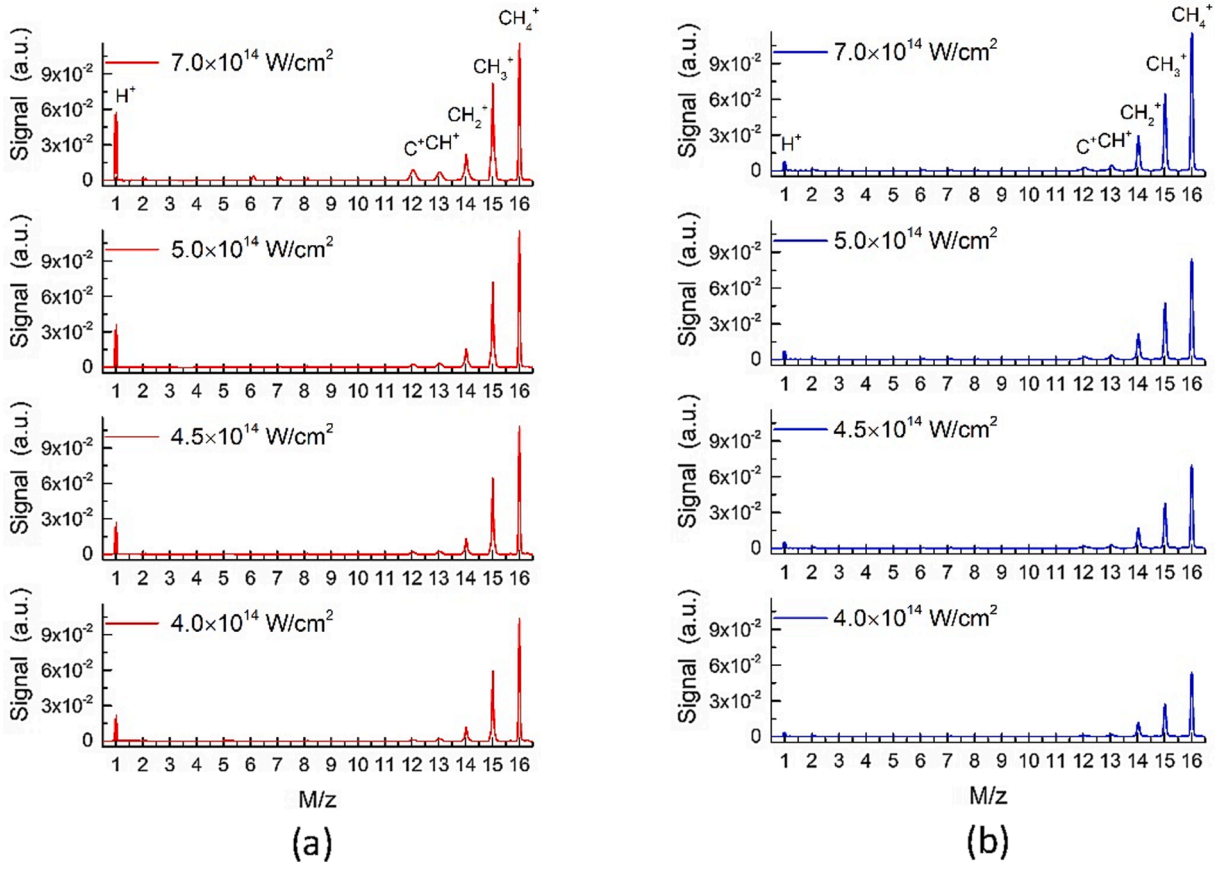

Fig. 4. (a) Ion TOF spectra as a function of the laser intensity for the dissociation of methane irradiated by 800 nm laser pulses for laser intensities ranging between 4 $\times 10^{14}$ W/cm^2 and 7 $\times 10^{14}$ W/cm^2. (b) Same spectra for irradiation with 400 nm laser pulses, obtained for the same intensities.

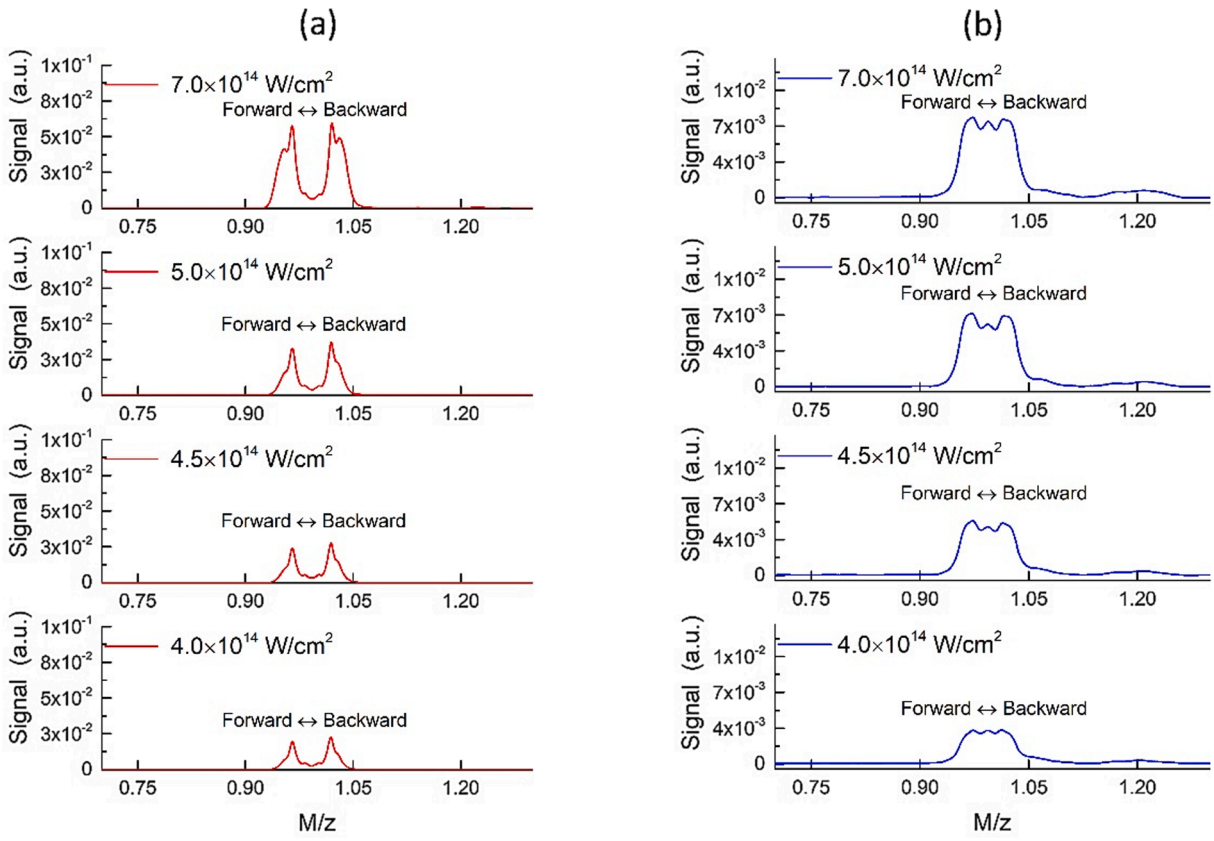

Fig. 5. H^+ fragment yields as a function of the laser intensity for dissociation of methane irradiated by (a) 800 nm and (b) 400 nm laser pulses.

Turning to the spectra acquired with the 400 nm field (Fig. 5(b)), once again, Coulomb explosion of the doubly charged unstable dications (CH_4^{2+}, CH_3^{2+}, CH_2^{2+}, CH^{2+}) should be expected to be the main source of the forward-backward H^+ peaks. However, in this case, the H^+ signal also exhibits a peak located between the Coulomb explosion driven peaks. Such a peak, is indicative of fragments with negligible kinetic energy, associated with ionization of atomic hydrogen, which is still possible at the higher laser intensities for the second harmonic wavelength.

A complete identification of the channels that give rise to the H^+ fragments is rather difficult. For example, the methane dication may contribute to the H^+ signal via the Coulomb explosion process: $CH_4^{2+} \rightarrow CH_3^+ + H^+$. This Coulomb explosion process would lead to the production of H^+ ions carrying a significant amount of kinetic energy. Both the $CH_4^{2+} \rightarrow CH_2^+ + H_2^+$ and the $CH_4^{2+} \rightarrow CH_3^+ + H^+$ Coulomb explosions would require a significant amount of energy to doubly ionize the methane molecule. The double ionization of the precursor would however be possible via the rescattering double ionization process [37]. More specifically, one can easily calculate that the ponderomotive energy acquired by the electrons can be higher than the ionization energy needed for the double ionization of CH_4 molecule, approximately (35–40 eV i.e. [38]), only for the upper end of the range of laser intensities used here and only for the 800 nm laser pulses. On the other hand, the second harmonic field is expected to significantly suppress the rescattering process. Hence, when the 800 nm laser field is concerned, we observe that the fastest H^+ peak in the spectrum appears as a shoulder at lower laser intensities (see Fig. 5(a)) and becomes a separate peak at higher intensities where the ponderomotive energies are high enough to ensure rescattering double ionization of methane. On the other hand, looking at Fig. 5(b) such a peak is absent in the case of the 400 nm laser field, even at the highest laser intensity, since the ponderomotive energy is not sufficient to induce the rescattering process in this case.

5. Conclusions

To conclude with, a comparative study was performed on the dissociation of methane irradiated by 800 nm and 400 nm ultrafast laser fields. The findings include the dissociation mechanisms, identified with the help of theoretical calculations for both laser wavelengths at relatively low intensities. As the laser intensity is increased, different fragmentation patterns emerge. Specifically, the presence of H^+ ions with significant kinetic energy suggests that Coulomb explosion of dications plays an important role for the case of strong 800 nm laser fields. On the other hand, this pattern is less pronounced for 400 nm laser fields, due to the suppression of the electron rescattering driven ionization mechanism. To the best of our knowledge, a systematic comparison of the dissociation mechanisms in methane for the two laser wavelengths used here, over such a broad range of intensities, has not been demonstrated in the literature before.

CRediT authorship contribution statement

Lazaros Varvarezos: Conceptualization, Visualization, Writing - original draft, Investigation, Data curation. **John T. Costello:** Conceptualization, Visualization, Writing - review & editing. **Conor Long:** Visualization, Writing - review & editing, Investigation, Data curation. **Alexander J. Achner:** Investigation, Writing - review & editing. **Rene Wagner:** Investigation, Writing - review & editing. **Michael Meyer:** Conceptualization, Visualization, Writing - review & editing. **Patrik Grychtol:** Conceptualization, Visualization, Writing - review & editing.

Declaration of Competing Interest

The authors declare that they have no known competing financial interests or personal relationships that could have appeared to influence the work reported in this paper.

Acknowledgments

LV acknowledges the award of a fellowship from the Education, Audio-visual and Culture Executive Agency (EACEA) Erasmus Mundus Joint Doctorate Programme under the EXTATIC Project No. 2013 0033. Work supported by Science Foundation Ireland Grant Nos. 16/RI/3696 and 19/FFP/6956 and associated with EU H2020 COST Action No. CA17126 (TUMIEE) and SEAI Grant No. 19/RDD/556. The authors wish to acknowledge the Irish Centre for High-End Computing (ICHEC) for the provision of computational facilities and support. RW and MM acknowledge funding by the Deutsche Forschungsgemeinschaft (DFG – German Research Foundation) –SFB-925 – project 170620586 at the University of Hamburg. AJA and MM acknowledge support by the Deutsche Forschungsgemeinschaft (DFG) through the excellence cluster "The Hamburg Center for Ultrafast Imaging (CUI)".

References

[1] E.D. Schulze, S. Luyssaert, P. Ciais, A. Freibauer, I.A. Janssens, J.F. Soussana, P. Smith, J. Grace, I. Levin, B. Thiruchittampalam, M. Heimann, A.J. Dolman, R. Valentini, P. Bousquet, P. Peylin, W. Peters, C. Rödenbeck, G. Etiope, N. Vuichard, M. Wattenbach, G.J. Nabuurs, Z. Poussi, J. Nieschulze, J.H. Gash, Importance of methane and nitrous oxide for Europe's terrestrial greenhouse-gas balance, Nat. Geosci. 2 (2009) 842–850.

[2] E.J. Dlugokencky, E.G. Nisbet, R. Fisher, D. Lowry, Global atmospheric methane: budget, changes and dangers, Philos. Trans. R. Soc. A Math. Phys. Eng. Sci. 369 (2011) 2058–2072.

[3] N. Stern, The Economics of Climate Change, Cambridge University Press, Cambridge, 2007.

[4] G.R. Smith, D.F. Strobel, A.L. Broadfoot, B.R. Sandel, D.E. Shemansky, J. B. Holberg, Titan's upper atmosphere: Composition and temperature from the EUV solar occultation results, J. Geophys. Res. Sp. Phys. 87 (1982) 1351–1359.

[5] Y.L. Yung, M. Allen, J.P. Pinto, Photochemistry of the atmosphere of Titan - Comparison between model and observations, Astrophys. J. Suppl. Ser. 55 (1984) 465.

[6] K. Codling, L.J. Frasinski, Dissociative ionization of small molecules in intense laser fields, J. Phys. B At. Mol. Opt. Phys. 26 (1993) 783–809.

[7] A.D. Bandrauk, Molecules in Laser Fields, in: Front. Chem. Dyn., Springer Netherlands, Dordrecht, 1995, pp. 131–150.

[8] J.H. Posthumus, The dynamics of small molecules in intense laser fields, Rep. Prog. Phys. 67 (2004) 623–665.

[9] S. Chelkowski, A. Conjusteau, T. Zuo, A.D. Bandrauk, Dissociative ionization of H_2^+ in an intense laser field: Charge-resonance-enhanced ionization, coulomb explosion, and harmonic generation at 600 nm, Phys. Rev. A 54 (1996) 3235–3244.

[10] A. Talebpour, K. Vijayalakshmi, A.D. Bandrauk, T.T. Nguyen-Dang, S.L. Chin, Phys. Rev. A 62 (2000), 042708.

[11] T. Seidema, M.Y. Ivanov, P.B. Corkum, Role of Electron Localization in Intense-Field Molecular Ionization, Chem. Phys. Rev. Lett. 75 (1995) 2819–2822.

[12] T. Zuo, A.D. Bandrauk, Charge-resonance-enhanced ionization of diatomic molecular ions by intense lasers, Phys. Rev. A 52 (1995) R2511–R2514.

[13] L. Robson, K.W. Ledingham, A. Tasker, P. McKenna, T. McCanny, C. Kosmidis, D. Jaroszynski, D. Jones, R. Issac, S. Jamieson, Ionisation and fragmentation of polycyclic aromatic hydrocarbons by femtosecond laser pulses at wavelengths resonant with cation transitions, Chem. Phys. Lett. 360 (2002) 382–389.

[14] M. Castillejo, S. Couris, E. Koudoumas, M. Martin, Ionization and fragmentation of aromatic and single-bonded hydrocarbons with 50 fs laser pulses at 800 nm, Chem. Phys. Lett. 308 (1999) 373–380.

[15] M. Castillejo, S. Couris, E. Koudoumas, M. Martin, Subpicosecond ionization and dissociation of benzene and cyclic alkanes at 800 and 400 nm, Chem. Phys. Lett. 289 (1998) 303–310.

[16] P. Tzallas, C. Kosmidis, K.W.D. Ledingham, R.P. Singhal, T. McCanny, P. Graham, S.M. Hankin, P.F. Taday, A.J. Langley, On the Multielectron Dissociative Ionization of Some Cyclic Aromatic Molecules Induced by Strong Laser Fields, J. Phys. Chem. A 105 (2001) 529–536.

[17] C. Kosmidis, P. Siozos, S. Kaziannis, L. Robson, K.W.D. Ledingham, P. McKenna, D. A. Jaroszynski, Interaction Mechanism of Some Alkyl Iodides with Femtosecond Laser Pulses, J. Phys. Chem. A 109 (2005) 1279–1285.

[18] K.W.D. Ledingham, D.J. Smith, R.P. Singhal, T. McCanny, P. Graham, H.S. Kilic, W. X. Peng, A.J. Langley, P.F. Taday, C. Kosmidis, Multiply Charged Ions from Aromatic Molecules Following Irradiation in Intense Laser Fields, J. Phys. Chem. A 103 (1999) 2952–2963.

[19] K.W.D. Ledingham, R.P. Singhal, D.J. Smith, T. McCanny, P. Graham, H.S. Kilic, W. X. Peng, S.L. Wang, A.J. Langley, P.F. Taday, C. Kosmidis, Behavior of Polyatomic Molecules in Intense Infrared Laser Beams, J. Phys. Chem. A 102 (1998) 3002–3005.

[20] V.V. Lozovoy, X. Zhu, T.C. Gunaratne, D.A. Harris, J.C. Shane, M. Dantus, Control of Molecular Fragmentation Using Shaped Femtosecond Pulses, J. Phys. Chem. A 112 (2008) 3789–3812.

[21] A.H. Zewail, Laser selective chemistry—is it possible? Phys. Today 33 (1980) 27–33.

[22] P. Hering, C. Cornaggia, Production of multicharged atomic ions from laser-induced multiple ionization of small molecules, Phys. Rev. A 57 (1998) 4572–4580.

[23] D. Mathur, C.P. Safvan, G. Ravindra Kumar, M. Krishnamurthy, Molecular-orientation effects in the dissociative ionization of CH_4 in intense laser fields, Phys. Rev. A 50 (1994) R7–R9.

[24] Z. Chen, X. Wang, B. Wei, S. Lin, R. Hutton, Y. Zou, Ionization and dissociation of methane in a nanosecond laser field, Phys. Scr. T144 (2011), 014065.

[25] C. Wu, Z. Wu, Q. Liang, M. Liu, Y. Deng, Q. Gong, Ionization and dissociation of alkanes in few-cycle laser fields, Phys. Rev. A 75 (2007), 043408.

[26] S. Wang, X. Tang, L. Gao, M.E. Elshakre, F. Kong, Dissociation of Methane in Intense Laser Fields, J. Phys. Chem. A 107 (2003) 6123–6129.

[27] M.E. Elshakre, L. Gao, X. Tang, S. Wang, Y. Shu, F. Kong, Dissociation of acetaldehyde in intense laser field: Coulomb explosion or field-assisted dissociation? J. Chem. Phys. 119 (2003) 5397–5405.

[28] X. Tang, S. Wang, M.E. Elshakre, L. Gao, Y. Wang, H. Wang, F. Kong, The Field-Assisted Stepwise Dissociation of Acetone in an Intense Femtosecond Laser Field, J. Phys. Chem. A 107 (2003) 13–18.

[29] M. Sharifi, F. Kong, S.L. Chin, H. Mineo, Y. Dyakov, A.M. Mebel, S.D. Chao, M. Hayashi, S.H. Lin, Experimental and Theoretical Investigation of High-. Power Laser Ionization and Dissociation of Methane, J. Phys. Chem. A 111 (2007) 9405–9416.

[30] R. Trebino, K.W. DeLong, D.N. Fittinghoff, J.N. Sweetser, M.A. Krumbügel, B. A. Richman, D.J. Kane, Measuring ultrashort laser pulses in the time-frequency domain using frequency-resolved optical gating, Rev. Sci. Instrum. 68 (1997) 3277–3295.

[31] W.C. Wiley, I.H. McLaren, Time-of-Flight Mass Spectrometer with Improved Resolution, Rev. Sci. Instrum. 26 (1955) 1150–1157.

[32] M.J. Frisch, G.W. Trucks, H.B. Schlegel, G.E. Scuseria, M.A. Robb, J.R. Cheeseman, G. Scalmani, V. Barone, G.A. Petersson, H. Nakatsuji, X. Li, M. Caricato, A.V. Marenich, J. Bloino, B.G. Janesko, R. Gomperts, B. Mennucci, H.P. Hratchian, J.V. Ortiz, A.F. Izmaylov, J.L. Sonnenberg, D. Williams-Young, F. Ding, F. Lipparini, F. Egidi, J. Goings, B. Peng, A. Petrone, T. Henderson, D. Ranasinghe, V.G. Zakrzewski, J. Gao, N. Rega, G. Zheng, W. Liang, M. Hada, M. Ehara, K. Toyota, R. Fukuda, J. Hasegawa, M. Ishida, T. Nakajima, Y. Honda, O. Kitao, H. Nakai, T. Vreven, K. Throssell, J.A. Montgomery, J.E. Peralta, F. Ogliaro, M.J. Bearpark, J.J. Heyd, E.N. Brothers, K.N. Kudin, V.N. Staroverov, T.A. Keith, R. Kobayashi, J. Normand, K. Raghavachari, A.P. Rendell, J.C. Burant, S.S. Iyengar, J. Tomasi, M. Cossi, J.M. Millam, M. Klene, C. Adamo, R. Cammi, J.W. Ochterski, R.L. Martin, K. Morokuma, O. Farkas, J.B. Foresman, D.J. Fox, in, Gaussian, Inc., Wallingford CT, 2016.

[33] J.A. Pople, R.K. Nesbet, Self-Consistent Orbitals for Radicals, J. Chem. Phys. 22 (1954) 571–572.

[34] R. McWeeny, G. Diercksen, Self-Consistent Perturbation Theory. II. Extension to Open Shells, J. Chem. Phys. 49 (1968) 4852–4856.

[35] Gaussian.com. 2021. Field [Accessed 8 January 2021].

[36] W. Meyer, PNO–CI Studies of electron correlation effects. I. Configuration expansion by means of nonorthogonal orbitals, and application to the ground state and ionized states of methane, J. Chem. Phys. 58 (1973) 1017–1035.

[37] P.B. Corkum, Plasma perspective on strong field multiphoton ionization, Phys. Rev. Lett. 71 (1993) 1994–1997.

[38] G. Dujardin, D. Winkoun, S. Leach, Double photoionization of methane, Phys. Rev. A 31 (1985) 3027–3038.